DRAINAGE THREE-PHASE FLOW RELATIVE PERMEABILITY ON OIL-WET CARBONATE RESERVOIR ROCK TYPES: EXPERIMENTS, INTERPRETATION AND COMPARISON WITH STANDARD CORRELATIONS

P. Egermann[1], K. Mejdoub[2*], J.-M. Lombard[2], O. Vizika[2] and Z. Kalam[3]
[1] Storengy – GDF Suez Group, [2] IFPEN, [3] ADCO, * now with Accenture

This paper was prepared for presentation at the International Symposium of the Society of Core Analysts held in Napa Valley, California, USA, 16-19 September, 2013

ABSTRACT

Three-phase flow data play a major role in the design of various E&P applications (gas injection, WAG, SAGD) and also in the context of gas storage activity (additional oil related to the conversion of depleted oil fields). Intermediate to oil-wet carbonate reservoirs comprise huge global oil reserves, and hence it is very important to characterize three-phase flow data to reduce current uncertainties.

This work is an experimental contribution to share new data sets of three-phase relative permeability (kr) obtained under drainage conditions (gas saturation increase) on different intermediate to oil-wet carbonate rock-types of two giant Middle East reservoirs. In each case, the ternary diagrams have been obtained through the numerical interpretation of displacement experiments conducted at various initial saturation conditions (from Swi to Sorw). Three-phase kr tables (functions of two saturations Sg and Sw) have been adjusted by trial-and-error method until a good history match was obtained for all the experiments (production data and pressure drop) with one unique set of tables. This process has led to very similar tables for each of the two rock-types in two different reservoirs.

Key findings are as follows:

- at a constant gas saturation, krg decreases with increasing amount of water
- krw depends on two saturations, excepted at low Sw
- kro depends on two saturations, excepted at low So, and the concavity of the isoperms is opposite, compared with the water-wet case. It leads globally to a reduced mobility of the oil phase under oil-wet context.

The general shape of oil isoperms is in good agreement with published results by Oak (1991), Petersen et al. (2008), and Weifeng et al. (2012) obtained on intermediate-wet and oil-wet sandstone samples. The results also show that the Stone's models fail in reproducing the experimental observations whatever the phase considered. Therefore, the current three-phase relative permeability models must be used with caution to simulate three-phase processes in oil-wet carbonate reservoirs. This is illustrated

through numerical simulations conducted on a five-spot gas injection pattern by comparing oil recoveries with raw and modeled three-phase flow data.

INTRODUCTION

Context

Three-phase flow data play a major role in the design of various E&P applications:

- gas injection processes including CO2, WAG (Shahverdi et al., 2011; Kalam, personal communications, 2013),
- steam injection during SAGD operations (Murtaza and Dehghanpour, 2012),
- gas storage activity in relation with the additional oil associated with the conversion of depleted oil fields (De Kok and Clemens, 2009).

Nevertheless, the experimental three-phase relative permeability data sets available in the literature are rather scarce to evaluate the applicability domain of available three-phase flow models implemented in reservoir simulators.

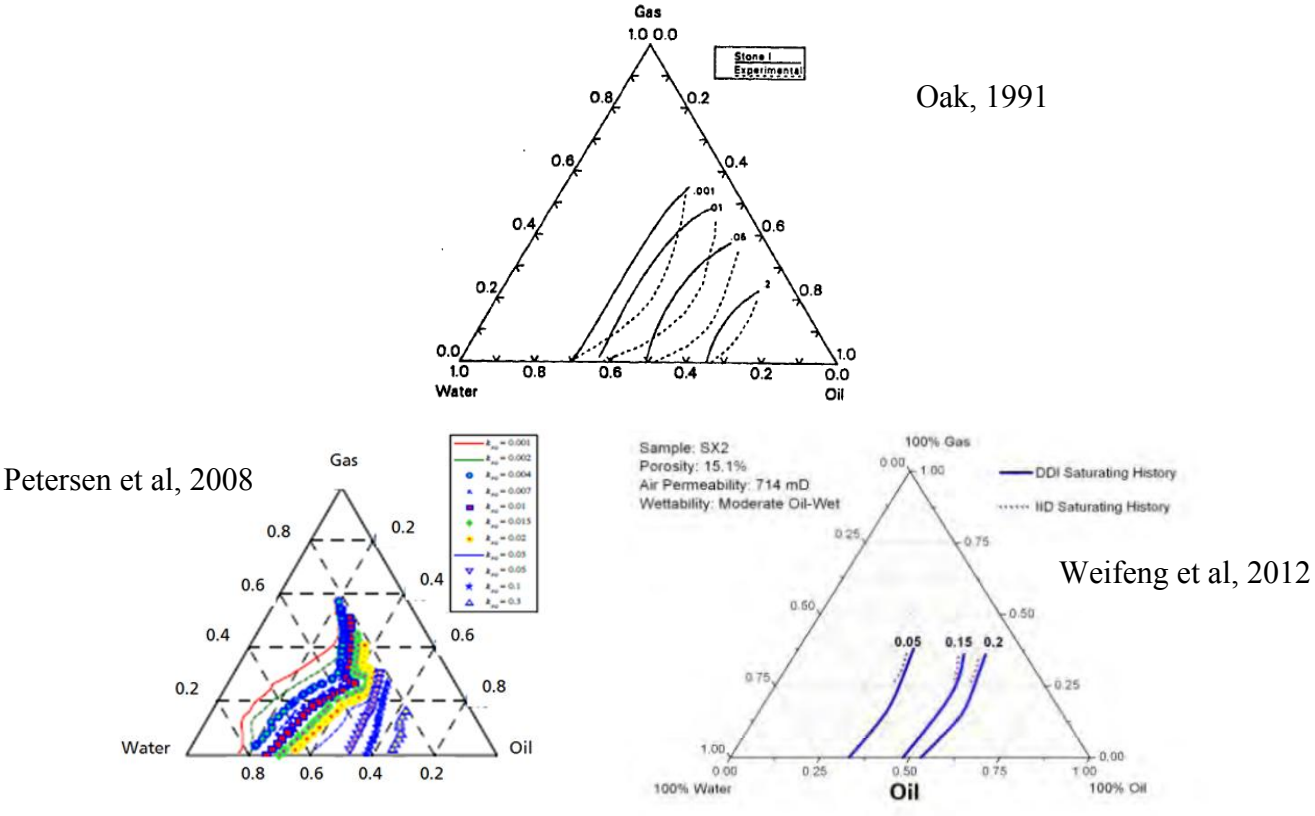

Figure 1: The oil isoperm concavity toward the oil phase, a common feature observed on all available three-phase data obtained on intermediate or mixed wettability

This is particularly true in the context of intermediate to oil-wet carbonate reservoirs although they represent huge global oil reserves. Figure 1 gathers the main available data on intermediate and mixed wettability cores (Oak, 1991: Berea sandstone;

Petersen et al., 2008: Statfjord sandstone; Weifeng et al., 2012: ShanXi sandstone). It is interesting to point out that all of them were exclusively acquired on aged sandstones. Whatever the data set published, the oil isoperms exhibit a characteristic shape with a pronounced concavity towards the oil phase whereas opposite trend is observed in water-wet cases (like what gives Stone 1 analytical model : top plot in Figure 1 with the solid lines - further illustrated in the discussion section).

This work consists in a contribution to share the three-phase flow data obtained under these specific wettability conditions but on carbonate cores. The manuscript is articulated in several parts. The first one is focused on the experiments that have been conducted to obtain enough data in order to investigate the three-phase flow region. The second part is dedicated to the numerical interpretation of the experimental data conducted to derive consistent three-phase relative permeability tables that enable to reproduce a whole set of experiments conducted on the same core. The next part proposes to discuss the results obtained on two different rock-types. The standard analytical models are first compared with these new data which have revealed their current limitations to reproduce the specific concavity of the oil isoperms under intermediate and oil-wet context. Finally large scale simulations based on a synthetic case (five spots) are presented to illustrate the implications of previously mentioned limitations in terms of additional oil recovery predictions.

EXPERIMENTS

Originally the three-phase flow experiments described hereafter were aiming at obtaining the residual oil contour after gas injection from various initial saturation states (Egermann et al., 2006). As the preparation of such experiments is complex and rather time consuming, it was decided to strengthen the monitoring in order to capture the transient evolution of the production curves in addition to the end-points. This has permitted to acquire additional information at limited extra cost and time about the three-phase flow functions. The same approach has been applied on two oil-wet carbonate rock-types from two giant Middle East reservoirs.

Core selection and preparation

All the experiments were performed under ambient conditions using two composite cores, aged at reservoir pressure and temperature, as described below, to obtain representative wettability conditions. Each of them was built with four individual plugs selected from the same carbonate homogeneous rock type (Table 1). The average properties are very similar in terms of porosity but quite different in terms of permeability (9.6 mD versus 3.2 mD) leading to different S_{wi} values obtained after desaturation using porous plate (12 bar applied with brine/docecane fluid system).

Table 1 : Petrophysical properties of the composite cores

Composite	S_{wi}	L	Porosity	K	Diameter
#	%	cm	%	md	cm
Reservoir A	8.5	30.65	28.4	9.6	4.9
Reservoir B	15.8	30.00	28.9	3.2	4.9

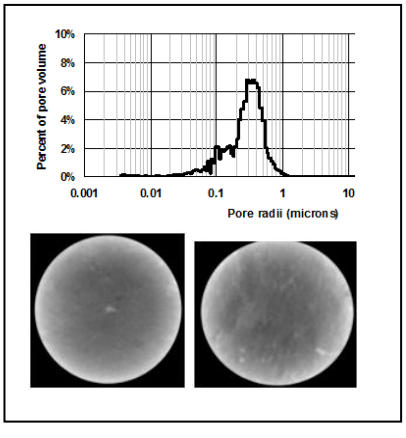

Table 2 : Plug properties for reservoir B, PSD and CT-scanner views

Plug	plug 1	plug 2	plug 3	plug 4	composite
L(cm)	7.34	7.53	8.03	7.1	30
K(mD)	3.6	2.8	2.9	3.6	3.2
Porosity (%)	28.9	28.6	29.0	29.1	28.9
Swi(%PV)	15.4	15.6	15.9	16.1	15.8

Special care was taken to use plugs with similar properties by checking initially the plug permeability to synthetic reservoir brine, comparing the mercury injection curves obtained on plug end pieces and analyzing each sample through X-ray CT scanner. This is illustrated in

Table 2 and associated figures (pore size distribution, PSD, and slice CT-scanner views) for the composite core built with reservoir B plugs.

Each composite was built following Huppler criterion (1969) to minimize plug permeability variations artefacts and mounted in a Hassler type cell. The core was then flooded with dodecane, cyclohexane and dead oil (cyclohexane was used to prevent any contact between oil and dodecane to avoid any risk of asphaltene precipitation). Pressure and temperature were respectively raised up above the bubble pressure and the reservoir temperature. Dead oil was finally displaced by live oil and the composite was aged during 4 weeks to restore the wettability. Each week, the composite core was flooded with one pore volume of recombined oil. After the aging process, the composite was successively flooded with dead oil, cyclohexane and dodecane. Pressure and temperature were lowered to laboratory conditions. During all this process, no brine was produced. This state (after Swi-setting and aging) was considered as the reference state prior to the gas injection experiments. Amott Index measured in companion plugs prepared exactly with the same protocol indicated a pronounced oil-wet type wettability (WI=-0.7 with no spontaneous water imbibition).

Fluids

Nitrogen (N2) was used as the gas phase, synthetic reservoir brine as the water phase and dodecane as the oil phase.

Experimental protocol for gas injections

For each composite, several gas injection experiments were conducted at various states to investigate the whole range of saturation in the ternary diagram. It has consisted of :

- One gas injection at Swi
- One gas injection at Sorw after waterflooding
- Two gas injections at intermediate saturation conditions

Gas secondary :

A medical CT-scanner was used to follow the evolution of the saturation profiles as a function of time during the gas injection experiment under secondary conditions. The oil and gas productions were recorded and CT-profiles were measured regularly during the experiment (Figure 2). In terms of gas monitoring, a returned beaker initially filled with water was installed at the outlet to accurately detect the gas production just after

gas breakthrough. Once the gas rate was high enough, the gas line was connected to a standard flowmeter. In all experiments, the displacements were run with a constant gas differential pressure (the outlet was maintained at atmospheric pressure) with the core composite mounted horizontally. A differential pressure of 1 bar was first applied, then 3 bar, and finally a high flow rate bump (DP = 8 bar) was applied (Figure 4).

Gas tertiary :
The composite core was first brought back to Swi by a succession of miscible displacements (methane, pentane, dodecane) after the gas injection at secondary condition. The permeability to dodecane under these conditions was quality controlled with the initial value. Then, brine was injected (Qw=10 ml/hr) to decrease the oil saturation down to Sorw. At the end of this phase, the gas was injected according to the procedure used under secondary conditions (DP=3 and 8 bar).

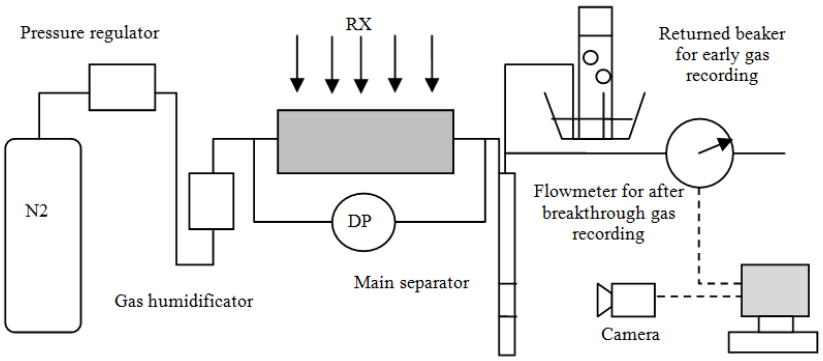

Figure 2: Experimental device

Gas intermediate 1 :

After the previous gas injection, a low salinity brine (20 g/l) was injected, followed by methane, pentane, methanol and isopropanol. This process was used to preserve as much as possible the restored wettability. Then, a low salinity brine and the simulated reservoir brine were successively injected until the core was 100% saturated with brine. An X-ray scanner profile was measured while the core was in a monophasic state (100% brine). Then, both brine and dodecane were simultaneously injected in the core (total flow rate equal to 20 ml/hr) in order to reach an intermediate saturation state (intermediate 1 in Figure 3). The gas injection was finally performed.

Gas intermediate 2 :

After this injection, a low salinity brine (20 g/l) was injected, followed by methane, pentane, methanol and isopropanol. Then, dodecane was injected until the core was fully saturated. A CT-profile was measured while the core was in a monophasic state (100% dodecane). By a succession of miscible displacements, it was possible to go back to 100% brine saturation. Then, a new steady state displacement was performed in order to reach another intermediate saturation state (intermediate 2 in Figure 3). At this state, a new gas injection was performed.

Results obtained

Figure 3 illustrates the average saturation pathways obtained from the sets of 4 experiments conducted on each reservoir. It can be observed that the displacements under Swi conditions follow a straight line indicating that no water was produced (black curves). The displacements under intermediate conditions follow rather similar pathways whatever the rock-type investigated. When departure is close to Swi (blue curves), oil production, then water and oil production is observed. When departure is close to Sorw (purple curves), water and oil production then mainly water production is observed. Under tertiary conditions (green curves), the pathways exhibit different shapes according to the reservoir considered. For reservoir A, oil production was recorded as an oil bank after water was produced. For reservoir B, oil production was recorded slowly but continuously from the starting of the injection.

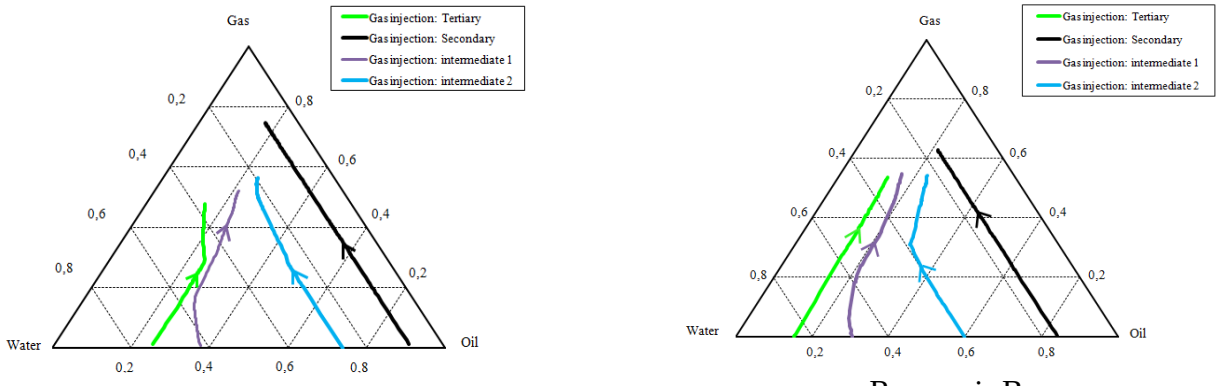

Figure 3: saturation pathways obtained in sets of experiments on reservoirs A and B

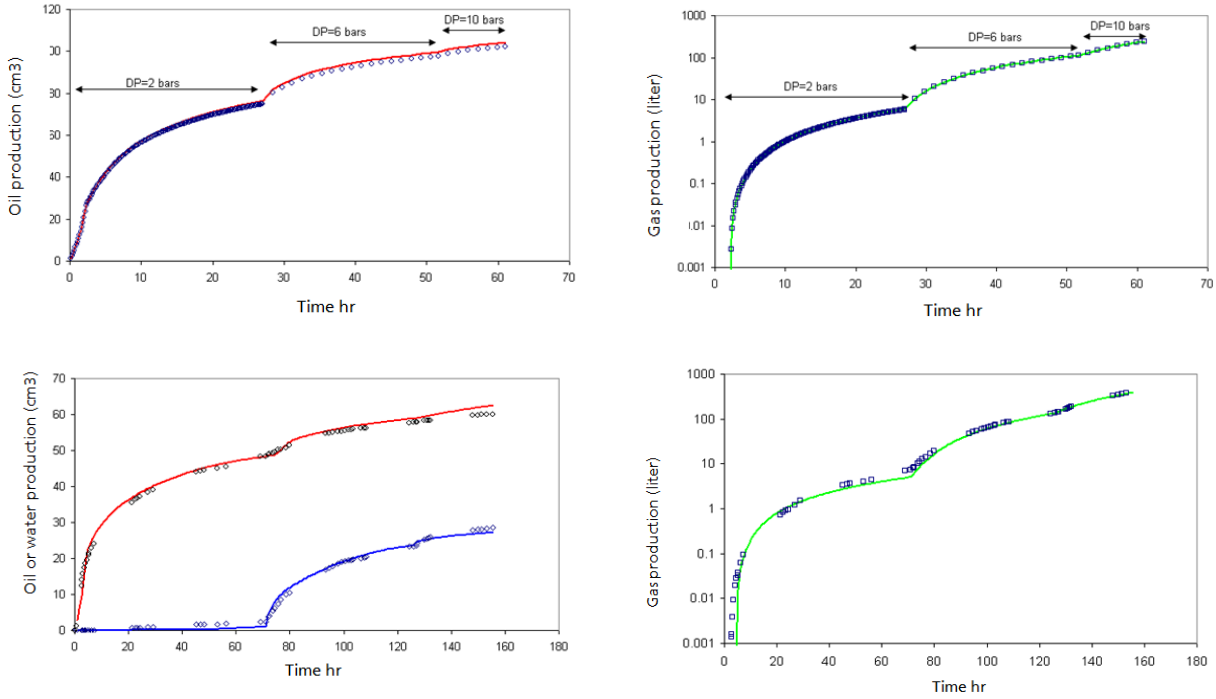

Figure 4: Examples of production curves obtained for reservoir B (top figures correspond to secondary conditions and bottom figures to intermediate 1). Color code (red=oil, blue=water and green=gas) – Blue points = experimental points

Examples of experimental production curves are displayed in Figure 4 (blue points) in addition to the simulated curves (solid lines) obtained after the history matching process (detailed in the next section).

HISTORY MATCHING AND RESULTS

In terms of numerical history matching of relative permeability, two cases can be distinguished depending on whether two or three phases are effectively mobile. Whatever the case, the simulations were conducted in 1D and account for gas properties evolution with pressure. The gridding in the x direction was built to respect the geometry of the samples used in the composite. 62 cells were used to describe the whole core. The drainage capillary pressure curve for the gas/oil fluid system was derived from mercury injection porosimetry data. As Sw decreases during gas injection experiment, a secondary drainage water/oil curve is needed. Available centrifuge data were used. In both cases, the raw curves, obtained on companion plugs with other fluid systems, were corrected using a J-function to take into account the plug variabilities in terms of permeability, porosity and also the effective interfacial tension values under ambient conditions with the fluid systems considered.

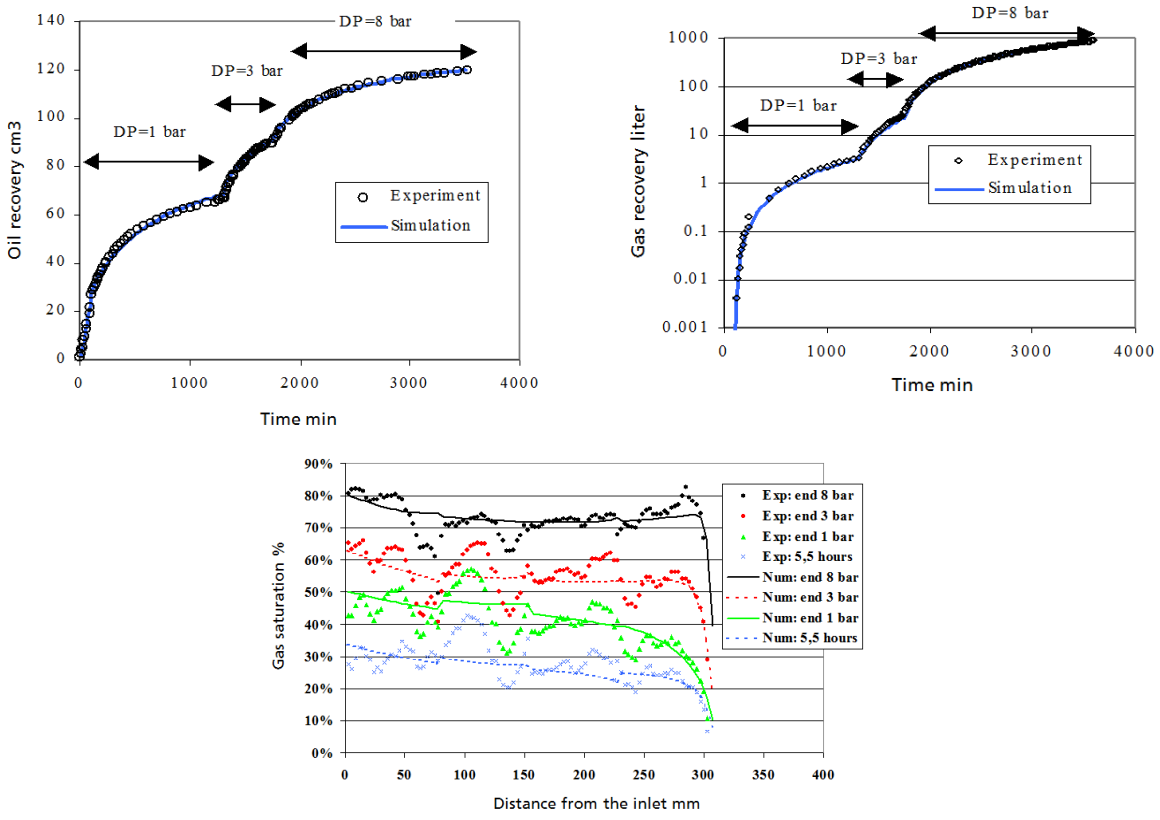

Figure 5: Secondary conditions history matching results for reservoir A

Gas injection at Swi (two-phase flow case)

The relative permeability curves were adjusted by trial-and error method until a good match was obtained in terms of oil production, gas production and local gas saturation measurements (Egermann et al., 2006). Finally, a very good agreement was found for both oil and gas recoveries as shown in Figure 5 for reservoir A and in Figure 4 for reservoir B (top plots). The gas breakthrough time was particularly well simulated considering the close match obtained at the early time for the gas production. The general shape of the profiles was well simulated especially the capillary end effect, which traps some oil at the outlet of the composite (Figure 5). Some variations of local saturation were also observed. This can be attributed to some local heterogeneity effects of the rock sample that cannot be reproduced using a single Pc-curve per sample but with local Pc (Egermann and Lenormand, 2005).

Gas injection with the three phases mobile

Three-phase relative permeabilities were introduced as tables, functions of two saturations (Sg and Sw). These three tables were adjusted by trial-and-error method until a good match was obtained for all the experiments with a unique set of tables. This process was done for each rock-type. The main advantage of this approach is that three-phase relative permeabilities can be adjusted directly with no need of specific three-phase analytical model. This enables to come up with "true" experimental relative permeability values.

The basics of the methodology has been proposed and detailed by Moulu et al. (1999). Two-phase relative permeability data are deduced from experiments where only two phases are mobile (steady state drainage water/oil used to set initial saturations in place and gas/oil drainage at Swi as described in previous section). When three phases are mobile, initial relative permeability values inside the ternary diagrams are first calculated directly from the experimental results after the gas breakthrough from Darcy's law, using average saturation and pressure drop. Then, depending on the differences between experimental observations and simulations with full account of capillary forces, these initial values of kr are modified until a good agreement is reached for all the experiments (4 per rock-type) using a unique set of tables.

The first difficulty in history matching three-phase flow experiments is that the modification of the kr value of one phase modifies the saturation state and therefore implicitly the kr values of the two other phases. This coupling varies depending on the phase considered. A modification of krg has little effect on the liquid productions and therefore on the saturation states whereas a modification of krw or kro can have a large impact on all phase productions. Therefore, it is recommended to adjust first the kr values of the liquid phases and then to tackle the modification of krg.

Reaching the level of consistency between 4 experiments using the same tables requires also several iteration steps. For example, the improvement of the history matching of one experiment can impact negatively the history matching of another experiment. Because saturation profiles exist in the core for given values of the average saturations during the gas flooding, some parts of the ternary diagrams impact the results of several experiments. At the end it was possible to find a satisfactory

history match for all the experiments as illustrated in Figure 4 and Figure 5 for few experiments among the 8 ones interpreted.

The final tables are presented in Figure 6. At a constant gas saturation, krg decreases with increasing amount of water. krw depends on two saturations, except at low Sw. kro depends on two saturations, excepted at low So and the concavity of the isoperms is opposite, compared to what is found in the water-wet case. It leads globally to a reduced mobility of the oil phase under oil-wet context which is in line with available data sets under intermediate wettability conditions (Figure 1). It is important to mention that these results are affected by some uncertainties although a specific care was taken to minimize them during the data acquisition (sufficient pore volume in miscible displacements to set reference states, volume and differential pressure recordings), the data correction (dead volumes as small as possible and accounted for in terms of volume shift and time lag) and the data interpretation phases.

DISCUSSION

Standard three-phase models comparison with the data sets obtained in this study

Most of the three-phase models developed are based on a combination between two-phase relative permeability functions (oil-water, krow, and gas-oil at Swi, krog). The first one was proposed by Stone (1973), version 1 and 2. Several improvements have been proposed later to modify the weights of kro from the two-phase functions according to the effective saturations (Baker, 1988), the wettability (Moulu et al., 1999; Temeng, 1991), the existence of film flow or blocking (Hirasaki's model described by Dietrich and Bondor, 1976; Blunt, 1999) and also to account for hysteresis (Larsen and Skauge, 1998).

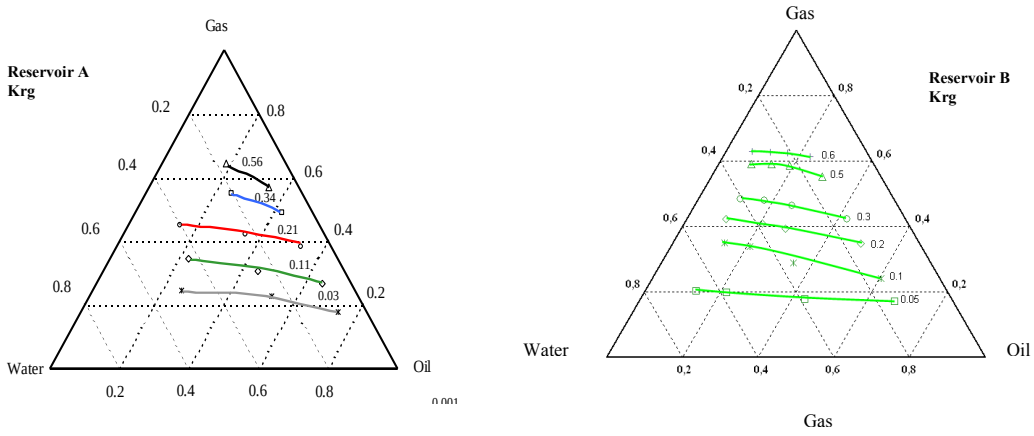

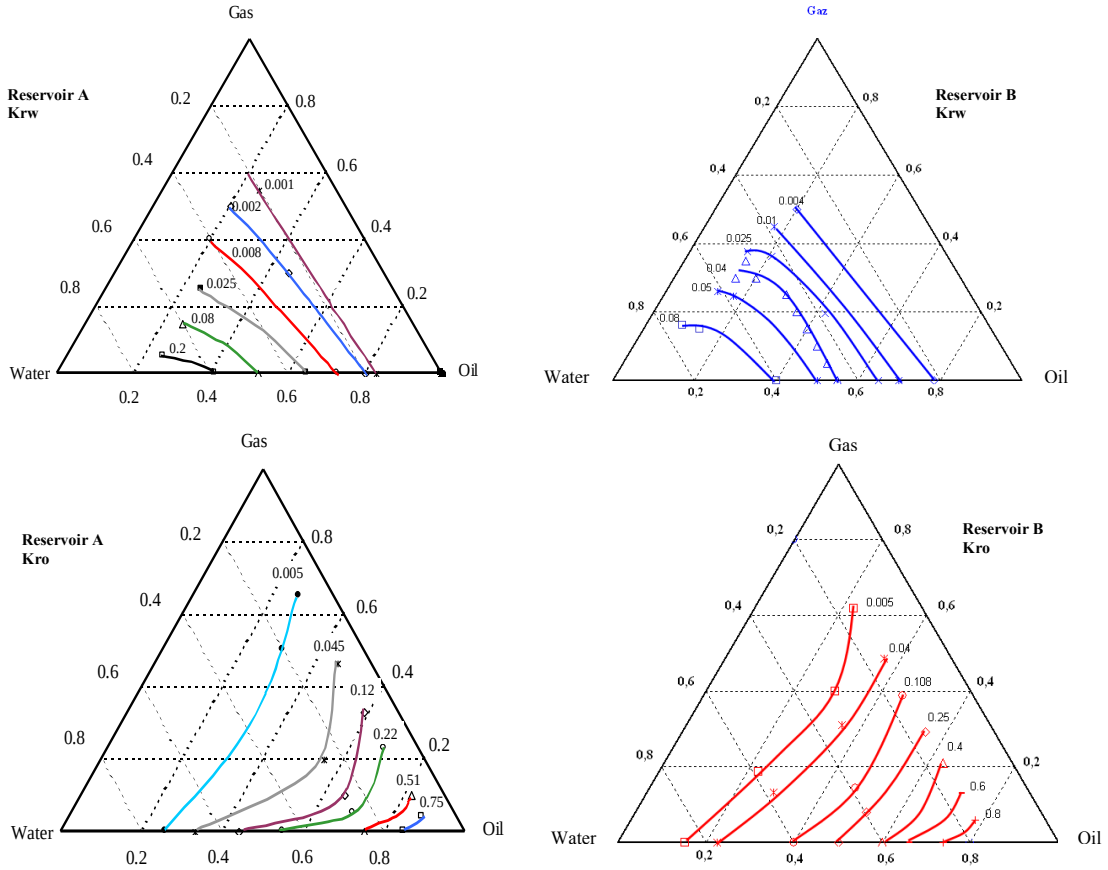

Figure 6: Three-phase isoperms obtained on reservoir A and reservoir B

An extensive comparison of these models has been conducted with the new experimental data sets. Figure 7 provides a synthetic view of the results of this analysis. The models with simple saturation weight functions do not enable to obtain concavity in the appropriate direction (Stone 1). Upon the model implemented in reservoir codes, the geometric approach (straight lines between krow and krog) provides the closest approximation (no concavity). Specific models developed to account for wettability, water blocking and film flows provides better shapes especially at low oil saturation with a change of concavity but they all exhibit the same behavior as the other models at high oil saturation. This is in line with the conclusions of other works based on a models comparison with Oak's data (Pejic and Maini, 2003; Ahmadloo et al., 2007; Behzadi and Alvarado, 2010; Weifeng et al., 2012).

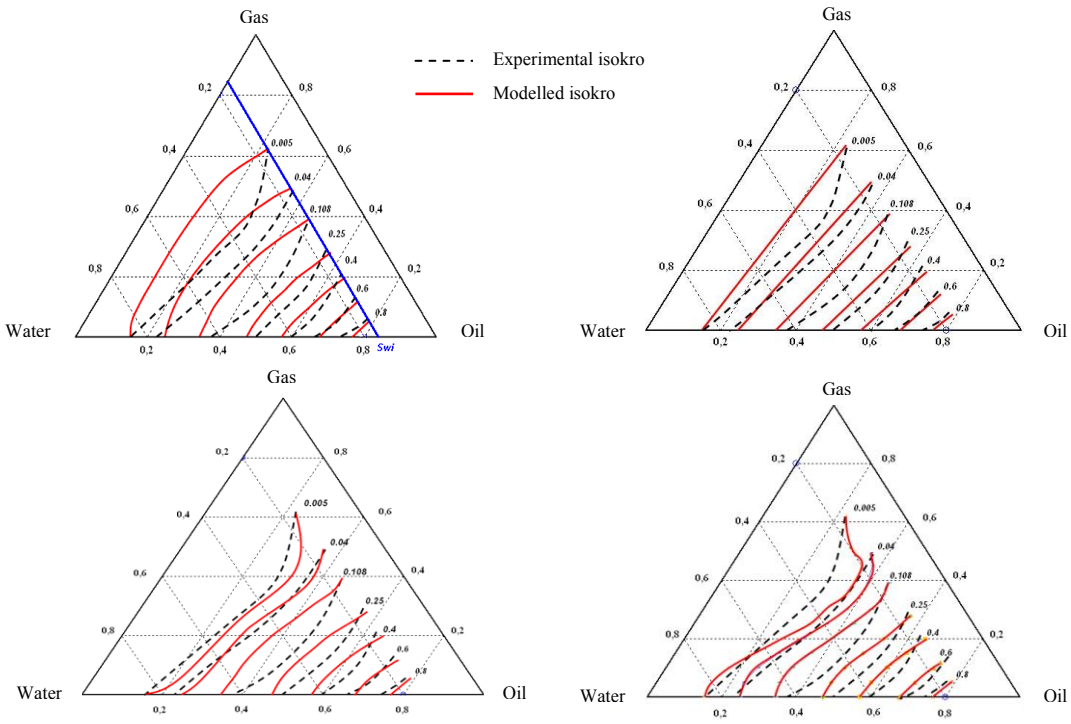

Figure 7: Top plots from left to right :comparison with Stone 1 and geometric interpolation – Bottom plots from left to right: comparison with Temeng and Hirasaki models

Impact on large scale studies

This study has been conducted by considering a five-spots configuration with several initial conditions in terms of saturation (35% and 50% water saturation) and various values of the kv/kh ratio. The permeability distribution has been obtained from a geostatistical realization with a correlation length equal to 250 m whereas the inter-well distance is equal to 450 m. The mean permeability value is 500 mD. The simulation was conducted for 6000 days and the numerical data set obtained after history match of the experiment was used as the reference case and compared with the results of the associated Stone1 model based on two-phase flow functions.

Small kv/kh value (0.001) leads to a better sweep of the reservoir (later gas breakthrough) because the gas gravity segregation is delayed and a more significant three-phase area is developed in the reservoir (Figure 8). In the case of 50% initial water saturation, the results indicate that Stone 1 overestimates the oil recovery (16%) comparing to the reference case, with the adequate oil isoperms concavity. At lower initial water saturation (35%), the discrepancy between the two approaches decreases significantly because in this case the saturation pathway follows a trajectory close to the two-phase flow data (along Swi) which are identical whatever the model.

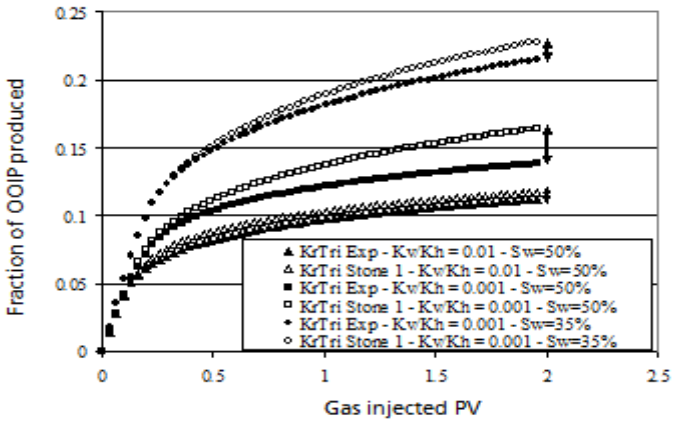

Figure 8: Comparison of the recovery curves according to the scenarios and three-phase data

CONCLUSIONS

The main contribution of this work is to provide new three-phase relative permeability data sets obtained on two intermediate to oil-wet carbonate rock-types (up to now only data from sandstones were available for similar wettability conditions). krg was found to depend on two saturations and is reduced at higher water saturation. krw also depends on two saturations except at low water saturation. The general shape of oil isoperms is in good agreement with published results by Oak (1991), Petersen et al. (2008), and Weifeng et al. (2012) obtained on intermediate-wet and oil-wet sandstone samples with a concavity towards the oil phase.

Evaluation of current three-phase models indicates that none was found adequate to reproduce the specific shape of oil isoperms under these wettability conditions. Large scale numerical simulations, conducted on a five-spot gas injection pattern, by comparing oil recoveries with raw and modeled three-phase flow data strongly suggest that the current three-phase relative permeability models must be used with caution to simulate three-phase processes in oil-wet carbonate reservoirs. For future works, the experimental data sets of three-phase data provided in this manuscript could help in the development of a new analytical model. This could also contribute to evaluate the ability of pore network modeling (Al-Dhahli et al., 2013) to reproduce the specific concavity of oil isoperms under intermediate wettability conditions that has been also experimentally identified in other publications.

ACKNOWLEDGEMENTS

We are grateful to ADCO and IFPEN for permission to publish these results and to S. Békri, J. Behot and P. Bretonnier for their contribution in the experimental work.

NOMENCLATURE

Kri : Relative permeability of phase i

kv/kh: permeability ratio (vertical versus horizontal)

REFERENCES

Ahmadloo F., Asghari K., Jamaloei Y.: “Experimental and theoretical studies of Three-phase relative permeability”, SPE 124538, ATCE, 4-7 October 2007, New Orleans.

Al-Dhahli A., Geiger S., van Dijke M.I.J.: “Three-phase pore-network modeling for reservoirs with arbitrary wettability”, SPE journal 147991, April 2013.

Baker L.E., "Three-phase relative permeability correlations", SPE 17369, Amoco Production Co., 1988.

Behzadi S.H., Alvarado V.: “Selection of Three-phase relative permeability model for mixed-wet reservoirs”, SPE 132849, Western Regional Meeting, 27-29 May 2010, Anaheim.

Blunt M.J., “An empirical model for model three-phase relative permeability”, SPE Journal 67950, December 2000.

De Kok J., Clemens T.: “Combined underground gas storage and increased oil recovery in a fractured reservoir”, SPE 129745, SPE Reservoir & Engineering Journal, December 2009.

Dietrich J.K. et Bondor P.L., "Three-phase oil relative permeability models", SPE 6044, 1976.

Egermann P. and Lenormand R.: “A New Methodology to Evaluate the Impact of the Local Heterogeneity on Petrophysical Parameters (KR, PC): Application on Carbonate Rocks”, SCA 2004-18 published in Petrophysics, vol. 46, n°5, Sept-Oct 2005.

Egermann, P., Robin, M., Lombard, J-M., Modavi, A. et Kalam, M.Z, Gas Process Displacement Efficiency Comparison on Carbonate Reservoir, SPE Reservoir Evaluation & Engineering 81577, December 2006.

Huppler, J.D. : “Waterflood Relative Permeability in Composite Cores” JPT, May 1969.

Larsen J.A., Skauge A.: “Methodology for numerical simulation with cycle-dependent relative permeabilities”, SPE Journal 38456, June 1998.

Moulu J-C., Vizika O., Egermann P., Kalaydjian F. :"A new three-phase permeability model for various wettability conditions", ATCE, 3-6 October 1999, Houston.

Oak M.J., “Three-Phase Relative Permeability of Intermediate-Wet Berea Sandstone”, Paper SPE 22599, presented at the 66th SPE Annual Technical Conference and Exhibition, Dallas, TX, October 3-6, 1991.

Pejic D. et Maini B.B., "Three-phase relative permeability of petroleum reservoirs", SPE 81021, SPE Latin Carribean Petroleum Eng. Conf., 27-30 April 2003, Trinidad.

Murtaza M., Dehghanpour H.: “Three-phase flow during steam chamber rise”, SPE 154287, IOR Symposium, 14-18 April 2012, Tulsa.

Petersen E.B., Lohne A., Vatne K., Helland J., Virnosky G. Oren P.-E., “Relative Permeabilities for two and three phase flow processes relevant to the depressurization of the Statfjord field”, SCA 2008-23, 29 Oct.-2 Nov., Abu-Dhabi.

Shahverdi H., Sohrabi M., Fatemi M., Jamiolahmady, Ireland S., Robertson G. : ‘’Evaluation of Three-Phase relative permeability models for WAG injection using water-wet and mixed-wet core flood experiments”, SPE 143030, EUROPEC/EAGE Annual Conference and Exhibition, 23-26 May 2011, Vienna.

Stone H.L.: “ Probability model for estimating three-phase relative permeability”, J Pet Technol, February 1970, pp. 214-218.

Temeng KO. Three-phase relative permeability model for arbitrary wettability systems. In: Proceedings of the Sixth European IOR-Symposium, May 1991, Stavanger.

Weifeng L., Zubo Z., Qingjie L., Desheng M., Kangyun W.: "Measurement of Three-phase relative permeabilities of various saturating histories and wettability conditions", SCA 2012-43, 27-30 August 2012, Aberdeen.